In these equations $\sigma_x(\sigma_y,\sigma_z)$ is the normal stress acting on a plane perpendicular to the x-(y-,z-) axis, ε_x is the normal dilatation in the direction of x, *i.e.*, the change of the spacing of two planes perpendicular to the x-axis, initially of unit spacing. τ_{yz} is the shear stress in the direction of y in a plane perpendicular to the z axis; it is equal to the shear stress in the z direction in a plane perpendicular to the y-axis ($\tau_{yz} = \tau_{zy}$). γ_{yz} is the displacement in the direction of y of two planes of unit distance normal to the z-axis; it is equal to the (relative) displacement in the z direction of two planes perpendicular to the y-axis ($\gamma_{yz} = \gamma_{zy}$).

If the equations are resolved with respect to the strain components ε and γ, six corresponding equations are obtained :

$$\left.\begin{aligned} \varepsilon_x &= s_{11}\sigma_x + s_{12}\sigma_y + s_{13}\sigma_z + s_{14}\tau_{yz} + s_{15}\tau_{zx} + s_{16}\tau_{xy} \\ &\vdots \\ \gamma_{yz} &= s_{14}\sigma_x + s_{24}\sigma_y + s_{34}\sigma_z + s_{44}\tau_{yz} + s_{45}\tau_{zx} + s_{46}\tau_{xy} \\ &\vdots \end{aligned}\right\} \quad (7/2)$$

The parameters c_{ik} are designated as moduli, the parameters s_{ik} as coefficients of elasticity.

8. *Simplification of the Equations of Hooke's Law as a Consequence of Crystal Symmetry*

The equations expressing Hooke's law can be greatly simplified if the symmetry of crystals is taken into account. Nine different groups are obtained, for which the matrices of the moduli of elasticity are shown in Table I. The table also indicates the distribution of the thirty-two crystal classes over these nine groups.

TABLE I

Matrices of the Moduli of Elasticity of Crystals Corresponding to Symmetry

Group 1. Class * C_1, S_2, triclinic system (twenty-one constants).

c_{11}	c_{12}	c_{13}	c_{14}	c_{15}	c_{16}
c_{12}	c_{22}	c_{23}	c_{24}	c_{25}	c_{26}
c_{13}	c_{23}	c_{33}	c_{34}	c_{35}	c_{36}
c_{14}	c_{24}	c_{34}	c_{44}	c_{45}	c_{46}
c_{15}	c_{25}	c_{35}	c_{45}	c_{55}	c_{56}
c_{16}	c_{26}	c_{36}	c_{46}	c_{56}	c_{66}

Group 2. Class C_s, C_2, C_{2h}, monoclinic system (thirteen constants).

c_{11}	c_{12}	c_{13}	0	0	c_{16}
c_{12}	c_{22}	c_{23}	0	0	c_{26}
c_{13}	c_{23}	c_{33}	0	0	c_{36}
0	0	0	c_{44}	c_{45}	0
0	0	0	c_{45}	c_{55}	0
c_{16}	c_{26}	c_{36}	0	0	c_{66}

* For the symbols of the various crystal classes cf. detailed treatises on crystallography.

TABLE I—*continued*

Group 3. Class C_{2v}, V, V_h, rhombic system (nine constants).

$$\begin{matrix} c_{11} & c_{12} & c_{13} & 0 & 0 & 0 \\ c_{12} & c_{22} & c_{23} & 0 & 0 & 0 \\ c_{13} & c_{23} & c_{33} & 0 & 0 & 0 \\ 0 & 0 & 0 & c_{44} & 0 & 0 \\ 0 & 0 & 0 & 0 & c_{55} & 0 \\ 0 & 0 & 0 & 0 & 0 & c_{66} \end{matrix}$$

Group 4. Class C_3, C_{3i}, hexagonal system (trigonal sub-group) (seven constants).

$$\begin{matrix} c_{11} & c_{12} & c_{13} & c_{14} & -c_{25} & 0 \\ c_{12} & c_{11} & c_{13} & -c_{14} & c_{25} & 0 \\ c_{13} & c_{13} & c_{33} & 0 & 0 & 0 \\ c_{14} & -c_{14} & 0 & c_{44} & 0 & c_{25} \\ -c_{25} & c_{25} & 0 & 0 & c_{44} & c_{14} \\ 0 & 0 & 0 & c_{25} & c_{14} & \frac{1}{2}(c_{11} - c_{12}) \end{matrix}$$

Group 5. Class C_{3v}, D_3, D_{3d}, hexagonal system (trigonal sub-group) (six constants).

$$\begin{matrix} c_{11} & c_{12} & c_{13} & c_{14} & 0 & 0 \\ c_{12} & c_{11} & c_{13} & -c_{14} & 0 & 0 \\ c_{13} & c_{13} & c_{33} & 0 & 0 & 0 \\ c_{14} & -c_{14} & 0 & c_{44} & 0 & 0 \\ 0 & 0 & 0 & 0 & c_{44} & c_{14} \\ 0 & 0 & 0 & 0 & c_{14} & \frac{1}{2}(c_{11} - c_{12}) \end{matrix}$$

Group 6. Class C_{3h}, D_{3h}, C_6, C_{6h}, C_{6v}, D_6, D_{6h}; hexagonal system (five constants).

$$\begin{matrix} c_{11} & c_{12} & c_{13} & 0 & 0 & 0 \\ c_{12} & c_{11} & c_{13} & 0 & 0 & 0 \\ c_{13} & c_{13} & c_{33} & 0 & 0 & 0 \\ 0 & 0 & 0 & c_{44} & 0 & 0 \\ 0 & 0 & 0 & 0 & c_{44} & 0 \\ 0 & 0 & 0 & 0 & 0 & \frac{1}{2}(c_{11} - c_{12}) \end{matrix}$$

Group 7. Class C_4, S_4, C_{4h}, tetragonal system (seven constants).

$$\begin{matrix} c_{11} & c_{12} & c_{13} & 0 & 0 & c_{16} \\ c_{12} & c_{11} & c_{13} & 0 & 0 & -c_{16} \\ c_{13} & c_{13} & c_{33} & 0 & 0 & 0 \\ 0 & 0 & 0 & c_{44} & 0 & 0 \\ 0 & 0 & 0 & 0 & c_{44} & 0 \\ c_{16} & -c_{16} & 0 & 0 & 0 & c_{66} \end{matrix}$$

Group 8. Class C_{4v}, V_d, D_4, D_{4h}, tetragonal system (six constants).

$$\begin{matrix} c_{11} & c_{12} & c_{13} & 0 & 0 & 0 \\ c_{12} & c_{11} & c_{13} & 0 & 0 & 0 \\ c_{13} & c_{13} & c_{33} & 0 & 0 & 0 \\ 0 & 0 & 0 & c_{44} & 0 & 0 \\ 0 & 0 & 0 & 0 & c_{44} & 0 \\ 0 & 0 & 0 & 0 & 0 & c_{66} \end{matrix}$$

Group 9. Class T, T_h, T_d, 0, 0_h, regular system (three constants).

$$\begin{matrix} c_{11} & c_{12} & c_{12} & 0 & 0 & 0 \\ c_{12} & c_{11} & c_{12} & 0 & 0 & 0 \\ c_{12} & c_{12} & c_{11} & 0 & 0 & 0 \\ 0 & 0 & 0 & c_{44} & 0 & 0 \\ 0 & 0 & 0 & 0 & c_{44} & 0 \\ 0 & 0 & 0 & 0 & 0 & c_{44} \end{matrix}$$

This arrangement can also be applied to s_{ik} with the following slight modifications :

In the Groups 4, 5 and 6 the relationship $s_{66} = 2(s_{11} - s_{12})$ replaces $c_{66} = \frac{1}{2}(c_{11} - c_{12})$; in Group 4, $s_{46} = 2s_{25}$ replaces $c_{46} = c_{25}$; in Groups 4 and 5, $s_{56} = 2s_{14}$ replaces $c_{56} = c_{14}$.

In each case the crystal is set up in such a way that any single axis of highest symmetry is the z axis, and a digonal axis, if any, the y axis of the system of co-ordinates. From the elastic parameters relative to this co-ordinate system it is possible to calculate directly the stresses (or deformations) in the co-ordinate axes and planes. If, on the other hand, it is desired to calculate the deformations from the stresses (or the reverse) for any directions or planes, then a new system of co-ordinates is based on these directions or planes, and the elastic parameters with reference to the principal system of co-ordinates must be transformed to this new system. The transformation formulæ are generally complex, and for further particulars the reader is advised to consult the detailed discussions of the subject referred to in the bibliography.

The following table of moduli of elasticity is obtained for an isotropic solid :

$$\begin{array}{cccccc} c_{11} & c_{12} & c_{12} & 0 & 0 & 0 \\ c_{12} & c_{11} & c_{12} & 0 & 0 & 0 \\ c_{12} & c_{12} & c_{11} & 0 & 0 & 0 \\ 0 & 0 & 0 & c_{44} & 0 & 0 \\ 0 & 0 & 0 & 0 & c_{44} & 0 \\ 0 & 0 & 0 & 0 & 0 & c_{44} \end{array}$$

in which $c_{44} = \frac{1}{2}(c_{11} - c_{12})$. The same arrangement is also valid for the coefficients s_{ik} with $s_{44} = 2(s_{11} - s_{12})$.

This matrix, which is independent of the choice of the co-ordinate system, contains only two independent parameters. The relationship between these quantities and the constants used in the literature of the strength of materials, namely, Young's modulus E, modulus of shear G, and Poisson's ratio μ, is given by the equations

$$E = \frac{1}{s_{11}}, \; G = \frac{1}{s_{44}} \; \mu = \frac{s_{12}}{s_{11}}.$$

From this it follows that $\mu = \dfrac{E}{2G} - 1$.

9. *Cauchy's Relations*

The equations of Hooke's law for the triclinic crystal contain twenty-one constants. The number is reduced to fifteen, however,

if the internal displacements of the constituent simple lattices are disregarded. This introduces six new relationships, known as the Cauchy relations, which formerly were obtained on the assumption that the central forces depended solely on the distance between the particles. The six equations are as follows :

$$c_{23} = c_{44},\ c_{56} = c_{14},\ c_{64} = c_{25},\ c_{31} = c_{55},\ c_{12} = c_{66},\ c_{45} = c_{36}$$

According to Born's theory these equations are valid if a crystal is so constituted that each particle is a centre of symmetry. Since this condition must persist for any distortion, relative displacements of the constituent simple lattices are excluded by virtue of the structure of the crystal.

Tables II and III contain the moduli of elasticity of various materials. It will be seen that the behaviour of the ionic crystals is in accordance with what would have been expected from their structure.

TABLE II

Validity of the Cauchy Relations for the Cubic Ionic Crystals

Material.	Moduli of elasticity in 10^{11} dyn/cm.^{2}.			References.
	c_{11}.	c_{12}.	c_{44}.	
(*a*) Cauchy relation $c_{12} = c_{44}$ demanded by theory.				
Sodium chloride . .	4·94	1·37	1·28	(2)
,, ,, . .	3·30	1·31	1·33	(2)
Potassium chloride .	3·70 3·88	0·81 0·64	0·79 0·65	(2) (3)
,, bromide .	3·33	0·58	0·62	(2)
,, iodide . .	2·67	0·43	0·42	(2)
(*b*) Cauchy relation $c_{12} = c_{44}$ not demanded by theory.				
Fluorspar . . .	16·4	4·48	3·38	(4)
Sodium chlorate . .	6·5	−2·10	1·20	(5)
Pyrite	36·1	−4·74	10·55	(4)

With metals, on the other hand, there is a very marked discrepancy between c_{12} and c_{44} even in cases where the validity of the Cauchy relation is demanded (Table III*a*) [cf. especially (1)]. Particular attention is drawn to this failure of the lattice theory in the case of metals. It may be that, owing to the ease with which they can be displaced, the valency electrons should be regarded as independent constituents of the lattice, since it is difficult to doubt Born's second

assumption relating to the stability of the lattice when deriving the Cauchy relations.[1]

For isotropic solids the six Cauchy equations are reduced to one : Poisson's equation $c_{11} = 3c_{12}$, so that in this case only a single constant survives. For Poisson's ratio the general value obtained

TABLE III

Validity of the Cauchy Relations for Metal Crystals

Material.	Moduli of elasticity in 10^{11} dyn/cm.^{2}.			References.	Poisson's ratio, μ.
	c_{11}.	c_{12}.	c_{44}		
(*a*) Cubic metals. Cauchy relation $c_{12} = c_{44}$ demanded if central forces assumed.					
Copper . .	17·0	12·3	7·52	(7)	0·34
Silver . .	12·0	8·97	4·36	(8)	0·37
Gold . .	19·4 18·7	16·6 15·7	4·00 4·36	(6) (8)	0·420
Aluminium .	$10{\cdot}8_2$	$6{\cdot}2_2$	$2{\cdot}8_4$	(6)	0·343
α-Brass (72% Cu)	14·7	11·1	7·2	(9)	—
α-Iron . .	23·7	14·1	11·6	(10)	0·280
Tungsten . .	51·3 50·1	20·6 19·8	15·3 15·1	(11) (12)	0·17

Material.	Moduli of elasticity in 10^{11} dyn/cm.^{2}.					References.	Poisson's ratio, μ.
	c_{11}.	$3c_{12}$.	C_{44}.	C_{13}.	C_{33}.		
(*b*) Hexagonal metals. Cauchy relations $c_{11} = 3c_{12}$; $c_{44} = c_{13}$ not demanded.							
Magnesium	5·65 . 10^{11} 5·94	6·96 6·09	1·68 1·14	1·81 2·03	5·87 5·94	(13) (14)	—
Zinc .	16·3 15·9	7·65 9·69	3·79 4·00	5·08 4·82	6·23 6·21	(15) (11)	0·33
Cadmium .	12·1 10·9	14·43 11·94	1·85 1·56	4·42 3·75	5·13 4·60	(15) (11)	0·30

is then $\mu = \frac{1}{4}$. With certain plausible assumptions, however, the constants of a quasi-isotropic crystal aggregate can be derived as mean values from the elastic parameters of the single crystal (cf.

[1] *Translator's footnote.*—According to the modern theory of metals (cf., *e.g.*, Mott and Jones, *Theory of Metals and Alloys*, or A. H. Wilson, *Theory of Metals*), the cohesive forces in metals are far from being central forces, and there is no reason to expect the validity of the Cauchy relations.

Section 81). If the Cauchy relations apply in this case, Poisson's equation is applicable to the crystal aggregate as a first approximation. Consequently, when measuring quasi-isotropic fine crystalline material, the deviation which is observed from the value for Poisson's ratio μ 1/4, provides a criterion for the validity of the Cauchy relations in the case of the single crystal. For this reason Table III contains the values for Poisson's ratio, determined on polycrystals, together with the parameters of the single crystal; the parallelism between deviation from Poisson's ratio of 1/4, and non-validity of the Cauchy relations, will be immediately apparent.

10. *Determination of the Elastic Parameters*

The elastic parameters are determined with the aid of the elastic constants of single crystals of various orientations. These elastic constants are, as for any solid: Young's modulus (E) and the modulus of shear (G), the definition of which applies without modification to crystals. [E = the tensile stress that would be necessary to double the length of the specimen, G = the shear stress that would develop on the periphery of a cylindrical specimen having a length and diameter = 1 when twisted round an angle of 1 radian (57·3°).] The elastic moduli of single-crystal specimens are obtained experimentally by the same methods as are used for testing isotropic solids. The determination of characteristic acoustic frequencies—a method of testing which recently has been much in use—offers particular advantages [transverse, longitudinal, torsional vibrations (16), (17); cf. (18) and (19) for the corrections which have to be applied in this case].

The theory of crystal elasticity yields two equations for $\frac{1}{E}$ and $\frac{1}{G}$ as functions of the angles formed by the axis of the bar with the axes of the crystal (orientation); the coefficients of these equations are the elastic constants s_{ik}. The problem consists in representing, as far as possible, the observed dependence of $\frac{1}{E}$ and $\frac{1}{G}$ upon the orientation by a suitable choice of the s_{ik}. A check for the resulting s_{ik} values is provided by their connection with compressibility. For the cubic compressibility K, which is independent of orientation, this relationship is as follows for the triclinic crystal: $K = s_{11} + s_{22} + s_{33} + 2(s_{12} + s_{23} + s_{31})$. It is customary, however, to measure the *linear* compressibility S (the change of length in certain directions under hydrostatic pressure), which is usually

dependent on direction. Only in the case of cubic crystals does a crystal sphere remain a sphere under hydrostatic pressure.

The following expressions give the theoretical dependence of E, G and S upon the orientation for cylindrical specimens of cubic and hexagonal crystals :

Cubic crystals :

$$\left.\begin{aligned} \frac{1}{E} &= s'_{33} = s_{11} - 2[(s_{11} - s_{12}) - \tfrac{1}{2}s_{44}] \\ &\qquad (\gamma_1^2\gamma_2^2 + \gamma_2^2\gamma_3^2 + \gamma_3^2\gamma_1^2) \\ \frac{1}{G} &= \tfrac{1}{2}(s'_{44} + s'_{55}) = s_{44} + 4[(s_{11} - s_{12}) - \tfrac{1}{2}s_{44}] \\ &\qquad (\gamma_1^2\gamma_2^2 + \gamma_2^2\gamma_3^2 + \gamma_3^2\gamma_1^2) \\ S &= s_{11} + 2s_{12} \end{aligned}\right\} \quad 10/1 \ldots 3$$

Hexagonal crystals :

$$\left.\begin{aligned} \frac{1}{E} &= s'_{33} = s_{11}(1 - \gamma_3^2)^2 + s_{33}\gamma_3^4 + (2s_{13} + \\ &\qquad s_{44})\gamma_3^2(1 - \gamma_3^2) \\ \frac{1}{G} &= \tfrac{1}{2}(s'_{44} + s'_{55}) = s_{44} + [(s_{11} - s_{12}) - \tfrac{1}{2}s_{44}](1 - \\ &\quad - \gamma_3^2) + 2(s_{11} + s_{33} - 2s_{13} - s_{44})\gamma_3^2(1 - \gamma_3^2) \\ S &= s_{11} + s_{12} + s_{13} - \gamma_3^2(s_{11} - s_{33} + s_{12} - s_{13}) \end{aligned}\right\} \quad 10/4 \ldots 6$$

In the case of the cubic crystals, $\gamma_1\gamma_2\gamma_3$ represent the cosines of the angles formed by the axis of the specimen with the three edges of the cube ($\gamma_1^2 + \gamma_2^2 + \gamma_3^2 = 1$); in the case of the hexagonal crystal only the direction-cosine γ_3 of the angle formed with the hexagonal axis appears, since the elastic properties have rotational symmetry with respect to the six-fold axis.

CHAPTER III

PRODUCTION OF CRYSTALS

Methods of obtaining large crystals have been greatly improved in the past twenty years, and we are to-day in a position to produce crystals of many metals and alloys in almost any size and form by a great variety of methods. In the following discussion of the new methods of growing crystals the processes have been grouped according to the state of aggregation from which crystallization takes place.

A. PRODUCTION OF CRYSTALS FROM THE SOLID STATE: THE RECRYSTALLIZATION METHOD

The term recrystallization usually means the renewed formation, generally at elevated temperatures, of the crystal structure of crystalline materials. Numerous experiments have shown that this renewal of the crystal structure does not occur with cast metals that are completely free from internal stresses (20, 21). If, however, a specimen which cannot recrystallize is plastically deformed, it acquires the capacity for renewing its texture. This recurs as a result of nucleus formation followed by the consumption of the old grains by the new ones.

In addition to this recrystallization due to deformation (" work recrystallization "), there is a phenomenon known as " grain growth " which leads to renewal of the texture, and which is exhibited by fine-grained recrystallization-structures or by finely powdered metal compressed at high temperatures. This process is not initiated by the formation of new crystal nuclei, but consists instead of the preferential growth of individual grains, in certain directions, at the expense of the others. It results from the instability caused by the higher surface energy of the polycrystal as compared with the single crystal.

As regards their structural mechanisms, both types of recrystallization are phenomena of atomic rearrangement.

11. *Recrystallization after Critical Plastic Deformation*

If recrystallization, after cold working, is used as a method for the production of large crystals, it will, of course, be necessary to ensure that the number of nuclei is kept to a minimum. Since this number

increases with the degree of strain, only small percentages of cold work should precede the annealing. A further necessary condition is that the deformation should be as homogeneous as possible so that a uniform capacity for recrystallization will result. To achieve this, a uniformly fine-grained structure is indispensable.

In order, therefore, to produce single crystals by recrystallization after cold working, it is necessary initially to obtain in the specimen, whether sheet, wire or tensile test bar, as fine and uniform a grain size as possible. If the required texture is not present in the initial material, it must be produced by previous recrystallization. A short annealing for about $\frac{1}{2}$ hour at a fairly low temperature after substantial cold working, or heating above a transformation temperature usually suffices for this purpose. After the specimens have been prepared in this way the most suitable percentage of working must be determined by subjecting them to small deformations of varying magnitude (usually elongations between $\frac{1}{2}$ and 4 per cent. are necessary), the utmost care being taken to exclude any additional strain, such as bending. The ensuing annealing treatment must also be carried out under very careful control with a view to reducing the number of nuclei to a minimum. For instance, annealing should begin at temperatures below that at which recrystallization starts, although for solid solutions they should be above the solubility limit. Metals that tend to oxidize easily should be annealed in a current of H_2 or *in vacuo*. By increasing the temperature very slowly (20–50° per day) one of the first nuclei formed may be induced to grow through the entire specimen, at the same time avoiding the formation of further nuclei. It is good practice to maintain a slight temperature gradient in the furnace (eccentric location of the specimens; if heating takes place under a stream of gas, the resultant temperature gradient suffices), since in this way the formation of further nuclei is avoided. Towards the end of the annealing period, which usually lasts for several days, the temperature can be increased more rapidly, and the operation is concluded by heating for a brief period just below the melting point (or a transformation temperature, a solidus line or a eutectic temperature) in order that small grains which generally are still present may be consumed by grain growth. Cooling should usually take place *inside* the furnace in order not to damage the crystals, which are particularly sensitive at high temperatures. Subsequent etching develops the boundaries of the newly formed crystals and ensures the removal of any small grains that may still be present on the surface. By comparing the specimens which have been subjected to varying degrees of working,

the critical working percentage at which crystals of maximum size can be obtained is determined (see Fig. 14).

In general, little of a positive nature can be said regarding the

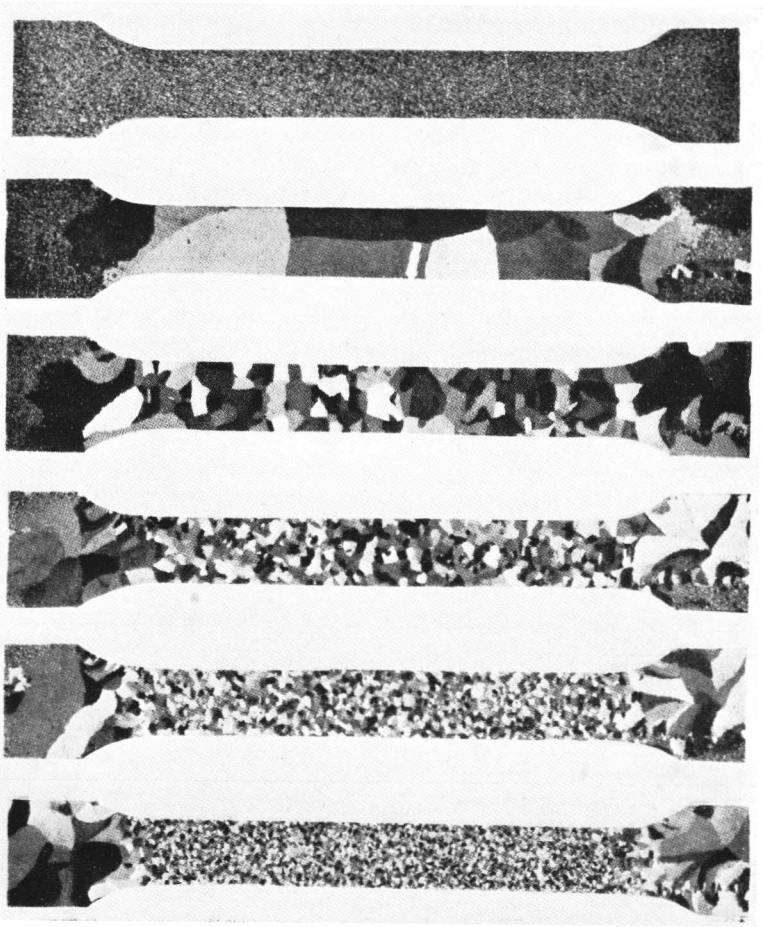

FIG. 14.—Recrystallization of Aluminium; Relationship between Grain Size and Plastic Strain.
(From top to bottom: 0, 2, 4, 6, 8 and 10% extension.) (22.)

yield of this process, since the growth of the crystals depends to a very large extent upon the composition and purity of the material used. In the most favourable cases, however, it may amount to almost 100 per cent. Arbitrary control of the orientation of the

crystals, *i.e.*, of the position of the lattice in the specimens, is impossible. As a rule the whole field of orientation can only be

TABLE IV

Crystal Production by Recrystallization after Critical Cold Working

Metal or alloy.	Pre-treatment, initial grain size.	Critical working, % elongation.	Annealing conditions.	References.
Mg	~120 grains/mm.²	0·2	From 300° to 600° C. in 6 days	(28)
Mg-solid solutions with Al, Zn, Mn, Al and Zn	Lengthy annealing just below eutectic temperature; 7–10% strain, followed by brief annealing	0·2–0·3	Anneal only in the range of homogeneous solid solution; daily increase in temperature 20–50° C.	(29)
Al~(99·5) *	~100 grains/mm.²	1·6	Start at 450° C.; increase temperature by 25°/day to 500° C. Then 1 hour at 600° C.	(22), (23)
Al-solid solutions with Zn (up to 18·6% Zn) and Cu	—	1–2	500–550° C.	(30), (31)
	—	1·5	In 6 days from 450° to 515° C.	(32)
Fe~0·13% C 0·4% Mn 0·02% Si 0·03% S 0·02% P	Pre-heat for protracted period at 950° C in H_2. About 120 grains/mm.²	3·25	A few days at 880° C.	(33)
Fe~0·10% C 0·4% Mn traces Si 0·021% S 0·021% P	—	2·75	4 days at 880° C.	(34)
Fe (Armco) 0·03% C 0·025% Mn traces Si 0·025% S 0·01% P 0·06% Cu	—	2·75	Increase from 530° to 880° in 4 days, then 2 days at 880° C.	(35) cf. also (36)

* The production of crystals of very pure aluminium (99·99 per cent.) has hitherto been attended by difficulties.

covered by increasing the number of specimens. In certain cases, however, this method fails, and the crystals obtained have similar orientations. This is due to the difficulty, and sometimes even the

impossibility, of obtaining a *fine-grained structure of random orientation* before the start of critical straining, and so avoiding the consequences of a preferred orientation.

The quality of the crystals obtained in this way is greatly influenced by that of the original material. Since all stresses are removed by the protracted anneal, it should be possible to satisfy requirements in regard to physical perfection. Owing to lack of experimental data it is not yet feasible to compare such crystals with those obtained by other methods.

The difficulties due to segregation, which occurs when crystals of solid solutions with a wide melting range are produced from the molten state, do not arise in the recrystallization method. Finally, the freedom which this method allows in the shaping of the specimen can be of great advantage in certain cases. It is a fundamental disadvantage of the work-recrystallization method that it involves plastic deformation, since brittle material is excluded from such treatment.

The main development of this method of growing crystals originates from (23) and (22) (cf. also 24). Details of the conditions employed by various authors will be found in Table IV. Apart from the metals mentioned in the table, the method has been adopted also with copper (25, 26) and β-brass; however, large crystals completely free from twins could not be produced in copper.

Using the same treatment it is possible to obtain from drawn tungsten wire those industrially important lamp filaments which consist of large crystals whose grain boundaries lie at small angles to the wire axis (27). The same texture can also be achieved without straining before the final anneal, if certain small additions are made to the base material. This method, however, should not be included among those described in the present section. It represents the transition to the methods of grain growth discussed in the following section.

12. *Crystal Production by Grain Growth*

The method of producing crystals by grain growth has been employed mainly in the case of tungsten. The so-called " Pintsch wires " are produced from a uniform and fine-grained tungsten powder which has been mixed with thorium oxide (approximately 2 per cent.) of maximum fineness; a bonding substance is added, and the mixture is then extruded through diamond dies to fine threads [(37), (38)]. After drying, these are moved at the rate of up to 1 mm. per second through a very hot and narrow zone (2500° C.) as a result of which the crystal growth starts at the end of the wire

and then proceeds continuously. The furnace consists of a few coils of a spiral of tungsten wire, heated electrically in a hydrogen atmosphere. A second method of effecting continuous local heating consists in passing a current through the sintered wire which is to be transformed into a crystal by moving it slowly over two adjacent contacts. There is still some doubt as to the function of the thorium oxide which must be added if the method is to succeed. The thickness of the crystals obtained in this way amounts to as much as 0·1 mm.

By another method (39), which can also be regarded as a typical grain-growth process, tungsten powder is pressed into bars at a pressure of 4000 kg./cm.^{2}, sintered and then heated for about an hour just below the melting point (3268° C.) in a moist hydrogen atmosphere. By this method it is sometimes possible to convert the entire bar into a single crystal. Although thermal instability is the cause of crystal growth, the water-vapour content of the protective gas also performs a very important function, the significance of which, however, is not yet fully understood. Grain growth can also be materially assisted by additions to the base material (*e.g.*, ThO_2) [(40), (41)].

B. PRODUCTION OF CRYSTALS FROM THE MOLTEN STATE

For the purpose of description, methods of growing large crystals from the molten state will be divided into two groups : processes in which solidification of the whole melt is suitably induced *in* the melting crucible, and those in which parts of the melt are made to solidify *outside* the crucible.

13. *Crystallization in the Crucible*

Tammann observed that if a melt of bismuth was cooled slowly in a glass tube, a single crystal of about 20 cm. length could be obtained (42). In succeeding years this process was perfected by a number of investigators. Glass vessels which had been drawn out at one end to a capillary tube were used. Solidification took place in the interior of a vertical tubular furnace containing two heating coils which could be switched on independently, thereby enabling solidification to start at the thinned-down end of the tube (43) : see also (44) to (47). The sketch of another melting vessel of glass which has been frequently used is shown in Fig. 15. The cavity *A* is charged with the metal to be melted and then drawn out at its front end *D* into a tube to which an air-pump is connected. After the parts *B* and *C* have been heated in an electric furnace to about 50–100° C. above the melting point of the metal, and the air has been exhausted from the entire vessel, the metal contained in *A*,

which projects from the horizontal furnace, is melted in a gas flame. The occluded gases are then driven off by shaking the molten mass, an operation which, for bismuth, must be prolonged for 1 hour. The furnace is now brought into a vertical position so that the metal flows down to the lower end, its quantity being so determined that finally a small amount of the melt remains in A, while all impurities, such as oxide skins, etc., are kept away from the actual melting chamber B. The vessel is now sealed at D, and crystallization is initiated by slowly lowering it (rate of lowering 4–60 mm. per hour). The purpose of the capillary between C and B, as in the case of the melting chamber mentioned above, is to allow only one of the initially formed crystals to penetrate to the chamber B in which crystallization actually occurs. The capillary works selectively, so that of the nuclei which first appear the one which ultimately develops is that for which the direction of maximum speed of growth encloses the smallest angle with the axis of the tube, as is shown in Fig. 16. It is seen clearly how crystals with small axial rates of growth are eliminated.

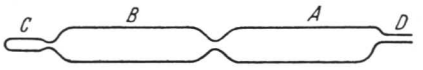

FIG. 15.—Sketch of Vessel for the Production of Metal Crystals [see (48)].

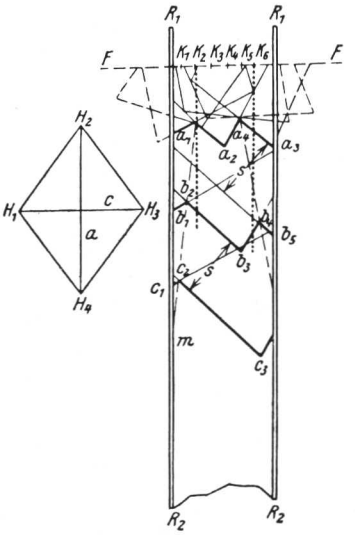

FIG. 16.—The Growth of Crystals in Tubes; Selection Based on Speed of Growth (49).

K_1–K_6: variously orientated crystal nuclei on the surface of the melt.

With a view to securing the maximum liberation of gas when producing crystals of metals and alloys of high melting point (copper, cobalt, nickel, the precious metals), vacuum furnaces were used repeatedly in which the melt, contained in a crucible made of carbon or alumina, was moved slowly through a graphite heating tube [(50), (51)]. The charge of the whole crucible can solidify in vacuum to large crystals (52) if provision is made for solidification to begin exclusively at one point, and for the heat to be withdrawn at a suitable speed mainly from this point, which may be, *e.g.*, a conical depression in the crucible. In this case the size of the

crystals is limited solely by the quantity of the material (size of the furnace). A copper crystal weighing 6 kg. was obtained by these means. Later the process was considerably improved [(53), (54)]. A high-frequency furnace was used, care being taken to avoid turbulence in the melt; the vacuum was improved to 1/100 mm. Hg; and, in particular, the orientation of the growing crystal was influenced. Indeed, whereas control of the orientation of the crystal is practically impossible with the crucibles already described (although it might conceivably be effected by tilting, at various angles, the capillary tubes at the lower end of the melting vessel, thereby exploiting the selective growth), the crucible design in use at present is such that the orientation of the crystal can be determined in advance by inoculation. For this purpose a small hole is drilled into the base of the graphite crucible, and into this hole a piece of crystal of the desired orientation is inserted. Heating is so regulated that only the upper portion of this crystal melts, so that crystallization proceeds from the seed crystal which serves as an artificial nucleus. It is, of course, always necessary to adjust the rate of cooling, or the speed at which the crucible is lowered through the furnace, to the speed of crystallization.

By this method single crystals have been produced from a large number of pure metals [Cu, Ni, Ag, Au, Mg, Zn, Cd, Hg (55, 56), Sn, Sb, Bi, Te] and alloys (α- and β-brass, Cu–Al, Cu–Sn, Au–Ag, Au–Cu, Au–Sn, Fe–Ni, Sb–Bi, Austenite).

If satisfactory crystals are to be obtained by this method care must be taken, by degassing the melts thoroughly, to avoid microporosity during crystallization. However, the segregation which occurs when producing the crystals of alloys cannot be avoided when crystallization proceeds from the melt. The material of the crucible must be chosen with the utmost care, both with a view to restricting contamination of the metal, and ensuring that the crystal will not be damaged when it is removed from the crucible. The production of completely undamaged, stress-free crystals by this method is in any case very difficult, and there has been no lack of experiments to ensure a still more careful handling of the crystal in the course of its production.

Of the methods evolved with this object in view there are four types [(57), (58)]. In the first method, the rod of metal which is to be converted into a single crystal is placed on a copper plate in which a temperature gradient has been produced by one-sided heating. First of all the rod is melted by adequate heating of the plate; owing to its surface tension and the presence of a thin oxide skin it

will retain its cylindrical shape. Crystallization is initiated at the cooler end of the plate by gradually decreasing the current. The orientation of the growing crystal can be influenced at will by contacting the melt with a " seed crystal " which has been placed at a suitable angle and which, of course, must not be completely melted down. By the second method the metal rod, which has been placed in a wide silica tube, is moved slowly through a narrow heating coil in a manner similar to that described in Section 12, melting and crystallization taking place consecutively. According to the third and simplest method the metal rod is put in a narrow cylindrical cavity bored into a copper block which is heated on one side only and which can be cooled under control. In both these cases it is possible to influence the orientation by the use of a suitable seed crystal. The fourth variant of the process (58) purports to improve upon the other three by eliminating also the stresses which emanate from the oxide skin. To this end the metal is melted down and solidified in a graphite channel placed in an evacuated silica tube which is moved slowly through the furnace. A current of purified hydrogen is passed through the tube. Each specimen is remelted several times before being brought into contact with the seed crystal. In this case the shape of the crystal is determined by the shape of the graphite channel. It is remarkable that hitherto this treatment should have been used only for bismuth, and (recently) tin (59).

So far we have described methods employed mainly for producing crystals from metals. Naturally they can also be adapted to the production of *salt crystals*. For instance, a furnace has been described (60) in which the melt is shaped like a plano-convex lens, in which the isotherms run parallel to the surface of the melt. Solidification proceeds uniformly from the bottom of the lens upwards. Large crystals have been produced in this way from sodium nitrate, potassium nitrate and sodium chloride, as well as from bismuth and zinc. By a further development of this method the internal stresses which lead to a tearing of the crystal can be eliminated (61). The following particulars are available of a method which has already been adopted for a large number of ionic crystals (sodium chloride, sodium bromide, potassium iodide, rubidium chloride and lithium fluoride) (62). A platinum tube, closed at the lower end and cooled internally by air, is immersed in the melt to the depth of a few millimetres. If the temperature has fallen to about 70° above the melting point of the salt, intensified cooling will cause crystallization to start on the platinum tube. When the

diameter of the hemisphere which has crystallized out (Fig. 17) amounts to about four times that of the platinum tube, the cooler is raised with the aid of a micrometer screw until the surface of contact between the crystallized spherolite (I) and the melt is composed of one crystal only. After this the greater part of the melt is made to crystallize by increased cooling (II). The operation is broken off before the crystal reaches the wall of the crucible. If this method is to be successful a period of growth of several hours will be needed for crystals averaging 3 cm. in size, and the temperature of the furnace (supply by accumulator battery) and of the cooling stream must be kept constant.

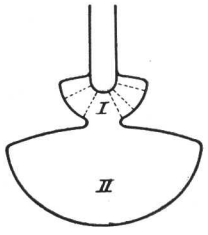

FIG. 17.—Illustrating the Production of Salt Crystals According to (62). Shape of the Crystal "Pears" Obtained in this Way.

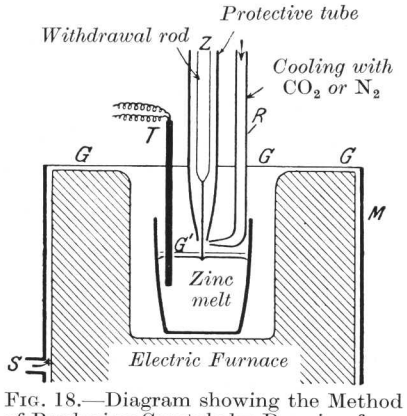

FIG. 18.—Diagram showing the Method of Producing Crystals by Drawing from the Melt. According to Czochralski [see (65)].

14. *Production of Crystals by Drawing from the Melt*

Czochralski (63) initiated a process which, although originally devised for the determination of the speed at which metals crystallize, was later much used for growing crystals. In this method a small rod (glass, clay or, better still, a seed crystal), immersed in the melt and serving as a centre of crystallization, is slowly and steadily raised. If the temperature of the melt is only slightly above the melting point, and if the rod is lifted slowly enough, there will adhere to it a small molten thread which crystallizes above the surface of the melt. The length of the crystals obtained in this way is limited by the dimensions of the apparatus : in shape they are approximately cylindrical.

Fig. 18 illustrates the type of equipment subsequently used

[(64), (65)] for producing crystal wires of a number of metals of low melting point. Through a small disc of mica (G'), perforated in the centre and weighted, a thread of molten metal is drawn, which is cooled just above the disc by a current of inert gas. In order to obtain crystals of maximum uniformity great care must be taken not only to maintain a constant melt temperature and constant speed of drawing and cooling but also to avoid vibrations. The diameter of crystal wires so obtained can be varied between about 0·2 and 5 mm., according to the conditions of heat removal. The requisite crystal orientations are obtained by using seed crystals with suitable lattice orientations. If intimate contact is maintained between melt and seed crystal (removal of the oxide skin), then the seed crystal will in most cases continue to grow. The role of the speed of drawing is still not fully explained. A speed of about 1 cm. per minute would appear to be smaller than the minimum rate of crystallization of the metals employed. This represents, of course, the natural upper limit of the speed of drawing.

By this method abundant material has been obtained for experiments, including crystals of Zn, Cd, Sn, Bi, Zn–Cd and Zn–Sn alloys.

The orientation of crystals produced in this way is always subject to slight but constant variations along the wire (66), caused, it is believed, by variations in the temperature gradient above the melt [cf. also (67)]. The maximum differences in orientation observed in zinc crystals 30 cm. long amounted to approximately 10°; however, if the experimental conditions were held constant they did not exceed about 2°.

The drawing method is also frequently used to-day for the production of *salt* crystals (68). In their case special cooling is usually unnecessary. The orientation of the growing crystal bars or "pears" can be materially influenced by inoculation.

The drawing process as described above cannot be used for reactive melts. For magnesium crystals, therefore, it is customary to employ a carbon tube which is immersed deep in the metal (the surface of which is covered with a protective layer) and is then slowly withdrawn (69). For protective purposes, this tube is enclosed in an iron tube, open at the bottom. This is provided at the top end with a cock which must be closed before withdrawal from the melt.

C. OTHER METHODS OF GROWING CRYSTALS

15. *Crystal Growth by Precipitation from Vapour*

When producing crystals from vapour it is customary to start with an existing seed crystal upon which the material is deposited.

In the case of tungsten the decomposition of the WCl_6 vapour is used. By one process (70) the tungsten hexachloride is reduced by hydrogen according to the equation

$$WCl_6 + 3H_2 = W + 6HCl.$$

Another method (71) makes use of the thermal decomposition of WCl_6 into its two components, which takes place at temperatures above 1500° C. In both cases a thin tungsten crystal (Pintsch wire) is used as a seed crystal, which, according to its orientation, grows into a 4-, 6- or many-sided crystal bar with a thickness of up to about 10 mm. By this method it is possible to deposit alternating layers of tungsten and molybdenum. In a similar manner crystals of Ta, Fe, Zr and Ti have also been precipitated from vapour (72).

The production of *zinc* and *cadmium* crystals by sublimation is described in (73). By this method six-cornered crystals with regular faces can be obtained without the use of seed crystals.

16. *Crystal Growth by Electrolytic Deposition*

This process, which is applied to tungsten (74), is similarly based on the use of a " Pintsch " wire as a seed crystal, the wire serving as a cathode in the axis of the cylindrical sheet of tungsten which constitutes the anode. Sodium tungstate forms the electrolyte, its decomposition being effected at 900° C. with a current density of 150 $mA/cm.^2$.

This concludes the description of methods for the production of crystals. Processes for growing salt crystals from the *solution* have not been included in this review; for information on this subject see the summary given in (75).

CHAPTER IV

DETERMINATION OF THE ORIENTATION OF CRYSTALS

The orientation of a crystal is the position of the lattice with reference to directions conveniently defined by the form of the crystal specimen. Whereas with crystals bounded by natural faces the position of the lattice is immediately obvious from the face angles (goniometrically measurable), with crystals of irregular shape it must be determined by special methods. Often it is only a question of determining the orientation of the lattice with reference to a *single* prominent direction of the crystal specimen (*e.g.*, the longitudinal direction of a cylindrical crystal rod) which is fixed by the angle it makes with the principal crystallographic axes. In the following pages we shall describe methods for determining the orientation of opaque crystals, with special reference to the investigation of metal crystals.

A. MECHANICAL AND OPTICAL METHODS

17. *Symmetry of Percussion-figures. Investigation of Light Reflected from Crystal Surfaces*

Orientation can be determined by mechanical tests only if a plane face is present on the specimen under investigation. The percussion-figure resulting from plastic deformation reveals the crystallographic nature of the plane normal (76).

Orientation can be determined much more precisely by investigating a crystal surface which, by etching, has been covered with crystallographically regular etch pits. These pits can also be replaced by a surface relief, consisting of microscopic or submicroscopic negative crystals, such as occurs, for instance, when metal crystals solidify from the melt. The first method of examining such a surface, *i.e.*, the determination by microscopical means of the shape of the etch pits on plane surfaces (77), is no more powerful than the percussion-figure method. The same is true of the " maximum lustre " method (78, 79), which uses the intensity of the light reflected from the etched surface. The specimen under investigation, exposed to oblique parallel light, is rotated around the axis of the microscope. From the number of alternations in intensity in the course of a complete revolution, the symmetry properties of the plane normal are deduced.

Whereas the above methods are restricted to certain simple cases and are dependent for their success on the presence of plane faces on the crystals, orientation can also be determined by investigating reflected light in the more general case [(80), (81)]. Since the principle is the same for both methods, the variant referred to in (81), which is the simpler and more commonly used of the two, will be described in detail. The crystal under investigation (we assume this to be a cylindrical rod) is placed in a hole drilled radially in a wooden sphere, and illuminated with parallel light (sunlight). The crystal is turned, together with the sphere, until a reflexion of maximum intensity is obtained. This direction is indicated by means of an adjustable mirror which is placed tangentially on the sphere, and which is also brought into the reflecting position, its point of contact with the sphere being marked. As a result of reflexions from several different faces a pole figure is obtained on the sphere, from which, assuming the interfacial angles of the crystal to be known, the position of the lattice in relation to the longitudinal axis of the crystal can be deduced. The only precaution needed is in regard to double reflexions, which, however, can be easily recognized. Direct readings of the desired angles can be obtained if the surface of the sphere bears a suitable network of meridians and parallel circles. It is obvious that this method can also be used to determine the crystallographic orientation of a polished surface; in this case the specimen must be attached tangentially to a pole of the sphere. A small systematic error arises in using this method owing to the fact that the normal of the reflecting crystal face does not pass through the centre of the sphere. The correction to be applied is discussed in (82), where particulars are also given of an extension of the method, using polarized light.

B. X-RAY METHODS

Very great possibilities for the investigation of orientation are opened up by the use of X-rays.

18. *The Diffraction of X-rays by Crystal Lattices*

A detailed account of the diffraction of X-rays by crystal lattices will be found in the relevant literature. Here we shall deal only with the features important to our special application—the determination of crystal orientations. The main progress which has resulted from the application of X-ray methods to the examination of solids has been in the determination of their internal structure. The distribution of the various structures among the elements of

the periodic system, together with numerical values of the lattice dimensions of the more important metals and of some ionic crystals,

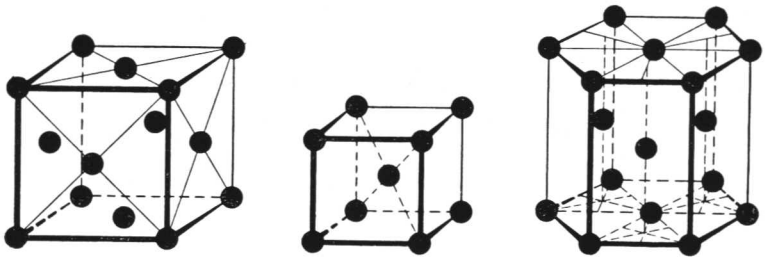

(*a*) Cubic face-centred. (*b*) Cubic body-centred. (*c*) Hexagonal close-packed.

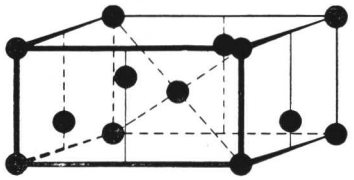

(*d*) β-Tin.

FIG. 19 (*a*)–(*d*).—Principal Metallic Lattices.

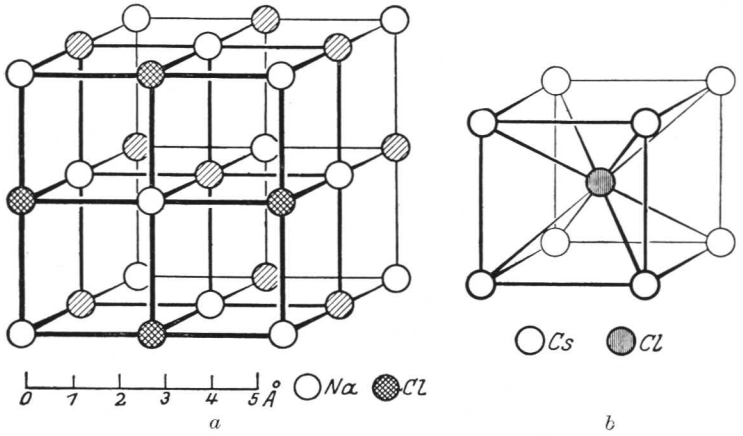

a *b*

FIG. 20.—Lattices of (*a*) Sodium Chloride and (*b*) Cæsium Chloride.

will be found in Tables XL–XLII at the end of the book. A few of the principal lattice types are shown in Figs. 19 and 20.

The diffraction of a beam of X-rays in a crystal can be regarded, according to Bragg, as reflexion of the rays from the different lattice

planes of the crystal. The reflexion of X-rays differs from ordinary optical reflexion (in which the angles of incidence and of reflexion are the same and lie in the same plane) in that it does not occur at *all* angles of incidence. It can occur only when the wavelength (λ) of the incident beam, the spacing (d) of the reflecting lattice plane, and the glancing angle [1] ($\theta/2$) satisfy the condition.

$$n \,.\, \lambda = 2d \,.\, \sin \theta/2 \text{ (Bragg's equation; } n = 1, 2, 3 \ldots)$$

Consequently a crystal at rest, if exposed to X-rays of a *single* wavelength, will not normally yield any reflexion, since none of the lattice planes will be at an angle to the ray which corresponds to d. There are two ways by which the requirements of Bragg's equation can be satisfied. (1) By using "white" X-rays the wavelength can be varied (Laue photographs); and (2) where monochromatic radiation is employed, by rotating the crystal (Bragg) the lattice planes can be made to pass through the reflecting position (rotation photographs). On the other hand, on irradiating a fine-grained crystal powder (polycrystalline material) the conditions for reflexion are satisfied even when the specimen is at rest, owing to the completely random orientation of the individual grains (Debye–Scherrer, Hull photographs).

(a) THE ROTATING-CRYSTAL METHOD

19. *Basic Formulæ*

The use of the rotating-crystal method for determining orientation is illustrated in Fig. 21 in terms of the geometry of the reference sphere [(83), (84) and (85)]. We observe the reflexion of the incident beam by the lattice plane (hkl) from which it is reflected at the glancing angle $\theta/2$. The plane normal, therefore, makes an angle of $(90–\theta/2)$ with the incident beam at the moment of reflexion, and the geometrical locus of the normal for all possible reflecting positions of the plane (hkl) is the circle of reflexion which is shown in the illustration as R_k. In the course of the rotation of the crystal about a geometrically important direction (longitudinal axis), which in Fig. 21 is chosen at right angles to the incident beam, the normal describes about the axis of rotation a double cone, whose intersection with the reference sphere is represented by the two parallel circles at polar distance ρ. The points at which the circle of reflexion intersects these two circles indicate the positions of the plane normal

[1] The glancing angle is the angle between the incident beam and the reflecting plane; consequently it is complementary to the angle of incidence of 90° used in optics.

at the moment of reflexion. Since the plane normal bisects the angle between reflected and incident beams, and is co-planar with them, the positions of the reflected rays are unequivocally determined. They make with the incident beam the angle of deviation θ, and therefore lie on a cone with vertical angle 2θ, having the incident beam as axis. The intersection of this cone with the photographic film gives the " Debye–Scherrer ring " of this plane, which represents the geometrical locus of the reflexion for all possible positions of the plane. This takes the form of a circle if a plate is used at right angles to the incident beam. However, if a cylindrical film is

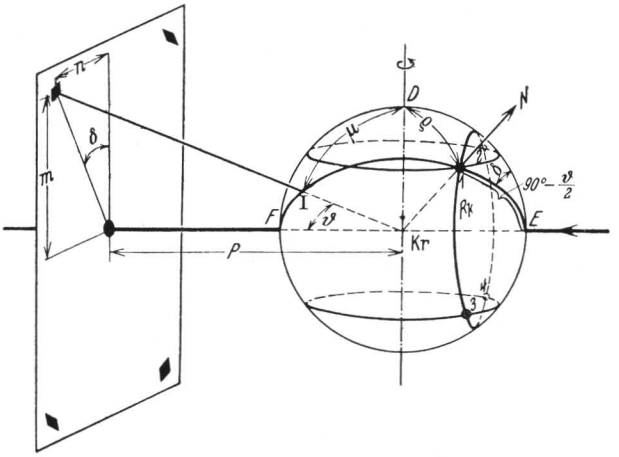

FIG. 21.—Determination of Orientation by Means of the Rotating-crystal Method.

employed, the axis of which would normally also be placed at right angles to the incident beam, then a curve of the fourth order is obtained. When the axis of the cylinder and the incident beam coincide, the curve degenerates into a circle; this in turn becomes a straight line when the film is laid out flat. Corresponding to the reflexion positions (1–4) of the reflecting plane, the reflected beams are also symmetrical in relation to the plane of the incident beam and axis of rotation, and to the " equatorial plane ", which is perpendicular to the plane of incidence.

If the film cylinder is perpendicular to the beam, the diagram contains the Debye–Scherrer rings of all the reflecting planes. The magnitude of the angle of deviation of X-rays on reflexion at a plane (*hkl*) is found by inserting the lattice-plane spacing (*d*) into

Bragg's equation (Section 6). The higher the indices and, consequently, the smaller the spacing of the lattice plane, the greater is the angle of deviation (θ) of the beam, which may be as much as 180°.

The intensity of the Debye–Scherrer rings depends on many factors, including primarily the structure-factor, which, however, will not be further discussed. Table V contains the indices of the lattice planes of the more important lattice types, arranged in order of increasing θ angles of the corresponding Debye–Scherrer rings.

TABLE V

Sequence of Debye–Scherrer Rings for some of the Metallic Lattices

Cubic.		Close-packed hexagonal.	
Face-centred.	Body-centred.	$c/a = 1{\cdot}633$ $(=2\sqrt{\frac{2}{3}})$.	$c/a = 1{\cdot}86$ (Zn).
111	110	$10\bar{1}0$	0002
200	200	0002	$10\bar{1}0$
022	112	$10\bar{1}1$	$10\bar{1}1$
113	022	$10\bar{1}2$	$10\bar{1}2$
222	013	$11\bar{2}0$	$10\bar{1}3$
004	222	$10\bar{1}3$	$11\bar{2}0$
313	213	$20\bar{2}0$	0004
024	004	$11\bar{2}2$	$11\bar{2}2$

The problem of orientation now consists in determining, by measurement of the positions of the reflexions on the diagram, the angle between the normal to the reflecting planes and the axis of rotation.

From the triangle $E1D$ (Fig. 21) we obtain first for the unknown angle ρ between face normal and axis of rotation the equation

$$\cos \rho = \cos \theta/2 \cos \delta \quad . \quad . \quad . \quad . \quad (19/1)$$

in which δ represents the angle between the plane of the incident beam and the axis of rotation, and that of the incident beam, normal, and reflected beam. The angle δ can be determined in various ways, according to whether the photograph has been recorded on a plate or cylindrical film. In the case of the plane shown in Fig. 21, the determination is very easy. δ can be measured either directly with a protractor, or calculated by measuring the distance between diffraction spots (reflexions). Let P be the distance

of the plate from the specimen, and n and m the rectangular co-ordinates of a reflexion (diffraction spot) with reference to the vertical and horizontal lines of symmetry of the diagram; it then follows that $tg\delta = \frac{2n}{2m}$ or, if the radius r $(= Ptg\theta)$ of the Debye–Scherrer ring is introduced, on which the four reflexions lie, then $\cos\delta = \frac{m}{r}$ and finally

$$\cos\rho = \frac{\cos\theta/2}{2P\,.\,tg\theta}\,.\,2m \quad . \quad . \quad . \quad . \quad (19/2)$$

Consequently, if the distance of the plate and the indices of the reflecting lattice plane (θ) are known, measurement of the distance $2m$ between two reflexions parallel to the axis of rotation will give the desired angle between plane normal and axis of rotation. Should it be necessary to determine orientations in large numbers, it is recommended that the relationship between ρ and $2m$ be represented in graphic or tabular form.

If the photograph is recorded on a cylindrical film of radius R, the axis of which is parallel to the axis of rotation of the crystal (perpendicular to the incident beam), then, if $2m$ represents the distance between reflexions (parallel to the axis of the cylinder), the following equation is obtained :

$$\cos\rho = \frac{1}{2\sin\theta/2}\cdot\frac{m}{\sqrt{m^2+R^2}} \quad . \quad . \quad . \quad (19/3)$$

Before we proceed to illustrate, by means of examples, the practical application of X-ray technique to the determination of orientation, it will be useful to offer some further observations on the method under discussion.

20. *Oblique Photographs*

In the first place, as may be seen from Fig. 21, it may happen that the plane normal no longer intersects the reflexion circle when the crystal is rotated. This will occur when the angle ρ is smaller than $\theta/2$. For $\rho = \theta/2$ the two parallel circles make contact with the reflexion circle at two points, and two reflexions are obtained on the vertical axis of the diffraction pattern, lying symmetrically above and below the equator. In the most frequent case of $\theta/2 < \rho < 90°$, the four reflexions referred to above will appear. As ρ increases, they will approach the equator of the Debye–Scherrer ring belonging to the plane, where ultimately for $\rho = 90°$, each pair of reflexions combines to form a single reflexion. Consequently the reflexions

for all those planes which belong to the zone of the axis of rotation will lie on the equator. In order to ensure that reflexions shall occur in all cases (including cases where $\rho < \theta/2$) the axis of rotation of the crystal is fixed at an angle $(90° - \theta/2)$ to the incident beam (Fig. 22). Symmetry relative to the equator disappears in these "oblique photographs" (83). The required angle ρ is obtained from the triangle $E1D$ by means of the relation

$$\cos \rho = \sin^2 \theta/2 + \cos^2 \theta/2 \cos \delta \quad . \quad . \quad (20/1)$$

δ can again be measured directly on the plate, or it can be calculated,

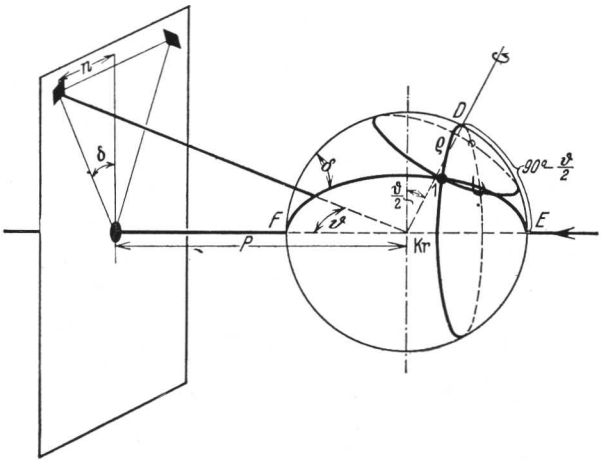

FIG. 22.—Determination of Orientation with the Aid of "Oblique" Photographs.

with the aid of the formula $\sin \delta = \dfrac{n}{P \,.\, tg\theta}$, from the distance $2n$ between the reflexions and the plate distance P.

If the angle between the axis of rotation and the incident beam is not $(90 - \theta/2)$, but β, then the equation which determines ρ is as follows:

$$\cos \rho = \cos \beta \sin \theta/2 + \sin \beta \cos \theta/2 \cos \delta \quad . \quad (20/2)$$

Oblique photographs are mainly important for use with crystals with unique planes (*e.g.*, hexagonal and tetragonal) whose position is important for the determination of the orientation of the crystal.

21. *Layer-line Diagrams*

A further observation concerns the special case in which the axis of rotation coincides with a crystal direction defined by simple

indices. The diagrams then possess certain specially simple features [namely, the arrangement of the reflexions on Polanyi " layer lines ",

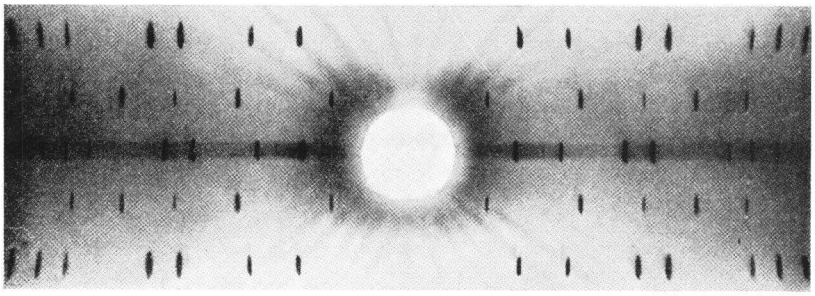

FIG. 23.—KBr Crystal : Layer-line Diagram Recorded on Cylindrical Film.

which appear as parallel straight lines when photographed on a cylindrical film, and as a set of hyperbolæ on a plate (Figs. 23 and 24)]. In discussing these diagrams we refer again to Fig. 21, in

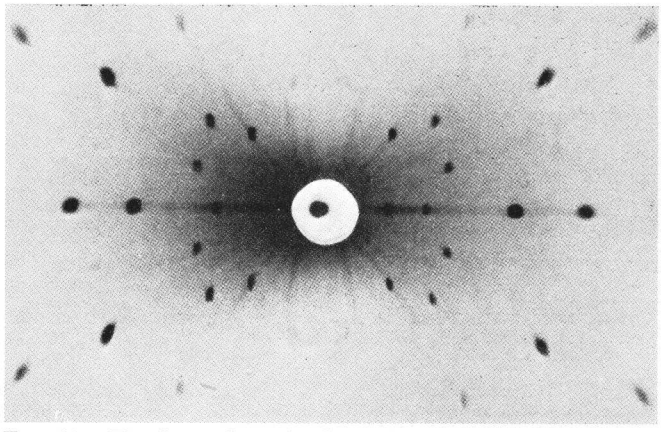

FIG. 24.—The Same Crystal : Layer-line Diagram Recorded on Flat Plate.

which the polar distance of the reflected beam is the angle μ. From the triangle FID we first obtain

$$\cos \mu = \sin \theta \cos \delta$$

from which, by substituting for $\cos \delta$ from equation 19/1, the following equation is obtained :

$$\cos \mu = 2 \sin \theta/2 \cos \rho \quad . \quad . \quad . \quad . \quad (21/1)$$

We next assume that the co-ordinates have been so transformed that the axis of rotation coincides with the new c-axis. The transformed index l' of the plane in question, relative to the new c-axis, indicates that the intercept on the axis amounts to $\frac{1}{l'}$ on this axis. Consequently l' equivalent lattice planes lie on the c-axis (axis of rotation) between two successive lattice points with the identity period J. For cos ρ Fig. 25 gives the expression

$$\cos \rho = \frac{l'd}{J}.$$

It then follows that for cos μ the equation is

$$\cos \mu = 2 \sin \theta/2 \frac{l'd}{J} = \frac{l'n\lambda}{J} \quad . \quad . \quad (21/2)$$

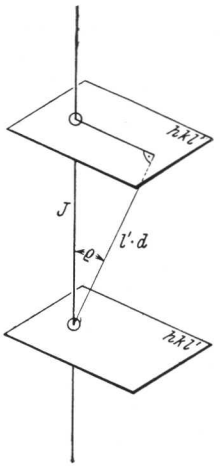

FIG. 25.—Method of Indexing Layer-line Diagrams (84).

It will be seen from this equation that for a given value of l' all reflected rays intersect the reference sphere at points on a parallel circle, at a distance μ from the pole, and that consequently the reflected rays lie on the surface of a cone with semi-vertical angle μ about the axis of rotation. The parallel circles corresponding to successive values of l' make equal intercepts on the axis of rotation so that the surface of the reference sphere carries a series of equidistant parallel circles. The index l' remains constant along each circle and increases by 1 on passing from one circle to the next.[1] The maximum index $l'_{\text{max.}}$ is derived from the condition $l'_{\text{max.}} \leq \frac{J}{\lambda}$ since cos $\mu \leq 1$. The index O corresponds to the equator of the reference sphere.

The intercepts of the cones of reflected rays belonging to the individual parallel circles with the film constitute the characteristic "layer lines". If the photograph is recorded on a cylindrical film with an axis which coincides with the axis of rotation, the film will be divided by the cones into circles, which will appear as straight lines when the film is laid out flat. If a plate is used, a set of hyperbolæ will appear with vertices on the axis of symmetry of the diagram parallel to the axis of rotation. Finally, if a cylindrical

[1] Provided that all reflexions on a layer line are not absent.

film is used with axis along the incident beam, the layer lines will be represented by an array of curves of the fourth order. This last type of photograph contains all the possible layer lines.

The significance of layer-line diagrams for the determination of crystal orientation lies in the fact that, from the spacing between the layer lines, or the vertices of the hyperbolae, the identity period parallel to the axis of rotation, and hence its crystallographic nature (when the lattice dimensions are known), can be readily ascertained (84). If for instance $2e_l$ is the space between the l^{th} layer lines, or between their vertices, then if R is again the radius of the cylinder of the film (or P the distance of the plate) :

$$\cot \mu_l = \frac{2e_l}{2R} \left(= \frac{2e_l}{2P} \right) \quad . \quad . \quad . \quad . \quad (21/3)$$

from which μ_l is calculated and can be inserted in

$$J = \frac{l \,.\, n \,.\, \lambda}{\cos \mu_l} \quad . \quad . \quad . \quad . \quad . \quad (21/2a)$$

The shortest identity period is obtained according to this formula if the order of the reflexion (n) in the Bragg equation is put equal to 1.

On the other hand, should the axis of rotation, as is more usual, not be a simple lattice direction, and thus be characterized by a large identity period, then the layer lines will fall so close together that it will no longer be possible to assign individual reflexions to separate layer lines.

22. *X-Ray Goniometer*

We conclude with a final observation on the subject of the complete determination of the orientation of the lattice in the specimen. The methods hitherto described yield the orientation in relation to one direction only. If the lattice orientation of the specimen is to be fully known, then either two such photographs must be obtained in different directions, or a photograph must be taken in an " X-ray goniometer " [(86), (87), (88)]. In this case rotation of the crystal is synchronized with movement of the film holder so that for each reflexion obtained the position of the specimen is known.

23. *Examples of the Determination of Orientation by the Rotating-crystal Method*

As a first example of the determination of orientation by X-ray methods we will work out the orientation of the axis of a rod-

shaped, cubic face-centred crystal with reference to the three axes of the cube. Fig. 26*a* shows the rotation photograph (flat plate, copper radiation $\lambda_{K\alpha} = 1{\cdot}54$ Å.) of an aluminium crystal, rotated about its longitudinal axis which is perpendicular to the beam. Owing to the distance from the plate (45·8 mm.) only the two innermost Debye–Scherrer rings ({111} and {200}) with the θ angles 38° 30′ and 44° 50′ are present. With the aid of the formula (19/2) or the

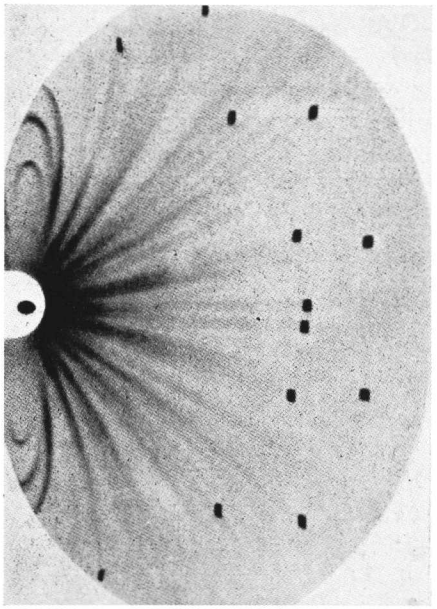

(*a*) Rotation photograph recorded on plate.

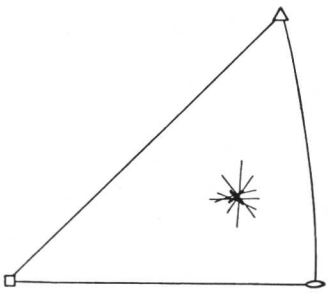

(*b*) Plotting of the arcs in the stereographic diagram.

FIG. 26.—Determination of the Orientation of an Aluminium Crystal.

equivalent graphical representation the corresponding ρ angles are now determined from the measured distances ($2m$) between reflexions. The above diagram gives :

$$2m_{(111)} = 2{\cdot}9,\ 21{\cdot}0,\ 52{\cdot}0 \text{ and } 70{\cdot}0 \text{ mm.}$$

from which it follows that

$$\rho_{(111)} = 87° 45',\ 74° 15',\ 47° 45' \text{ and } 24° 45'$$

and $2m_{(200)} = 20{\cdot}2$ and $54{\cdot}0$ mm.

i.e., $\rho_{(200)} = 78° 15'$ and $56° 45'$.

Although two angles suffice to determine the orientation of the longitudinal axis, there is close agreement (between the different values), and, as will be apparent from the stereographic diagram

shown in Fig. 26*b*, this increases the degree of accuracy of the final result. The arcs in Fig. 26*b* are plotted in the first place with reference to the normals of two reflecting planes (*e.g.*, in the present case two cubic axes); arcs having the known ρ angles are then described round these. The crystallographically equivalent normals from which the remaining angles are to be plotted (cf. Fig. 11)—in this case the four angles with the cube body diagonals—will appear from the initial rough determination of orientation (intersection of the first two circles to be described). By taking advantage of the known symmetry of the crystal it is always possible to complete the plotting of the orientation in the same basic triangle. The mean values for

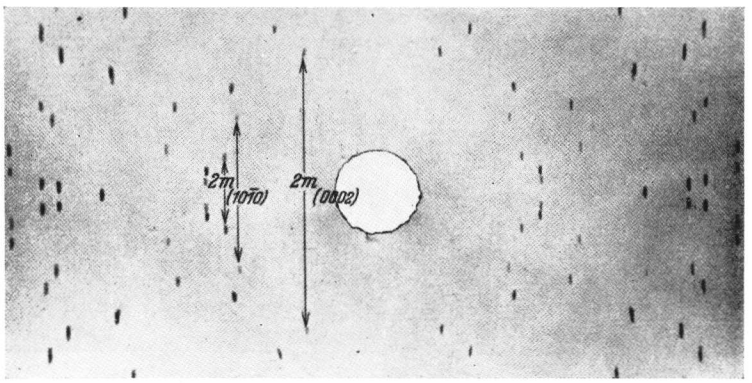

FIG. 27.—Rotation Photograph of a Zn Crystal (Cylindrical Film).

the angles between the axis of the rod and the cubic main axes in the present example are found ultimately to be 78°, 56° 30′ and 36°.

In our next example we will determine the orientation of a hexagonal crystal (zinc) in the form of a wire with the aid of a rotating-crystal photograph on a cylindrical film perpendicular to the beam (Fig. 27). In this case the orientation will be specified by the angle χ between the wire axis and basal plane, and the angle λ between wire axis and the nearest digonal axis type I. The reflexion from the basal plane appears in the case of zinc on the innermost Debye–Scherrer ring, that of the prism planes of type I on the next ring (Table V); the corresponding θ angles are 36° 20′ and 39° 10′ for copper radiation.

It follows from $2m_{(0002)} = 36{\cdot}4$ mm., with the aid of equation (19/3) ($2R = 57{\cdot}3$ mm.) that the angle between wire axis and hexagonal axis is $\rho_{(0002)} = 30°\ 40'$. From $2m_{(10\bar{1}0)} = 9{\cdot}4$ and 19·8 mm. for the reflexions from the prism planes type I we obtain

the two angles $\varrho_{(10\bar{1}0)} = 76°$ and $60°\ 20'$ between wire axis and two digonal axes type II (normals to the prism planes type I). Once again there is agreement between the different values of the orientation deduced from these figures. By forming an average in the stereographic net we find that

$$\chi = 60°$$
$$\lambda = 63°\ 30'.$$

Finally, from the two layer-line diagrams in Figs. 23 and 24 we will determine the crystallographic nature of the axis of rotation of a rod of potassium bromide.

From the distances between the layer lines

$$2e_1 = 13{\cdot}7 \text{ and } 2e_2 = 30{\cdot}0 \text{ mm.}$$

the diameter of the camera being 57·3 mm., it follows from the formula (21/3) that the angles

$$\mu_1 = 76°\ 30' \text{ and } \mu_2 = 62°\ 20'.$$

Further, we obtain from (21/2a), with $n = 1$, a value of 6·63 for J from the first layer line, and of 6·65 for J from the second layer line; giving a mean value for $J = 6{\cdot}64$ Å. Comparison with the measurements for the KBr lattice (Table XLII) shows that the rotation axis was parallel to the cubic axis of the crystal.

The same result is arrived at from an evaluation of Fig. 24. The distances between the vertices of pairs of hyperbolae are $2e_1 = 7{\cdot}8$ and $2e_2 = 16{\cdot}6$ mm., which, for a plate distance of $P = 16{\cdot}0$ mm., gives a value of $76°\ 20'$ for μ_1 and of $62°\ 30'$ for μ_2, and so similarly indicates the cubic axis as the axis of rotation.

(b) LAUE METHOD

Compared with the methods described above for determining the orientation of crystals by the use of monochromatic radiation, the method based on Laue photographs is relatively unimportant. It can, however, be used with advantage to determine the crystallographic orientation of the face normals of plate-shaped crystals.

There is a general similarity in the appearance of Laue photographs, in so far as the individual reflexions corresponding to the different wavelengths lie on curves which are conic sections, and always include, as vertex, the point of incidence of the direct beam, which is perpendicular to the plate. All beams reflected from the planes of a zone constitute the generators of a circular cone about

the zone axis, whose intercept with the photographic plate gives the conic sections known as " zone circles ".

As a rule the specimen is held between the plate, which is perpendicular to the incident beam, and the X-ray tube. So long as the angle between the zone axis and the direct beam is less than 45° the zone circles appear on this plate as ellipses, which become parabolas when the zone axis is inclined at 45°. If the axis of the zone is more steeply inclined to the incident beam, then the zone circle becomes one branch of a hyperbola. In this case the zone also appears as one branch of a hyperbola on a photographic plate placed *between* X-ray tube and specimen, but the vertex does not coincide with the point of incidence of the direct beam, as in the case of the first plate. Finally, if the zone axis is perpendicular to the incident beam, the cone degenerates into a plane which intersects both plates in straight lines passing through the point of incidence of the direct beam. Both transmission (89) and back-reflexion Laue photographs can now be used to determine crystal orientation. As already mentioned, by this method (in which the specimen is not rotated), the position of the lattice is determined in relation to a system of co-ordinates in space and not in relation to a direction only (namely the direction of rotation) as is the case when using the rotating-crystal method.

24. *Example of the Determination of Orientation by Laue Photographs*

The method can be illustrated by two examples, the examination of a magnesium crystal by means of a transmission photograph [according to (90)] and of an aluminium crystal by means of a back-reflexion photograph. The two diagrams are shown in Figs. 28*a* and 29*a*. The zone circles are easily recognized in both pictures. Since the individual reflexions are due to various unknown wavelengths, it is not at first possible to assign them to definite lattice planes. On the other hand, it is easy to ascertain the position of the reflecting lattice plane with reference to the direction of the incident beam (*i.e.*, the direction of the normal to the crystal plate).

Let S_1 or S_2 be the distance of each reflection from the point of incidence of the primary beam, then the angle of deviation θ_1 of the X-ray beam is obtained for the transmission photograph from $tg\theta_1 = \frac{S_1}{P_1}$, the deviation θ_2 for the back-reflexion photograph from $tg\ (180° - \theta_2) = \frac{S_2}{P_2}$, which in P_1 or P_2 represent the distances from

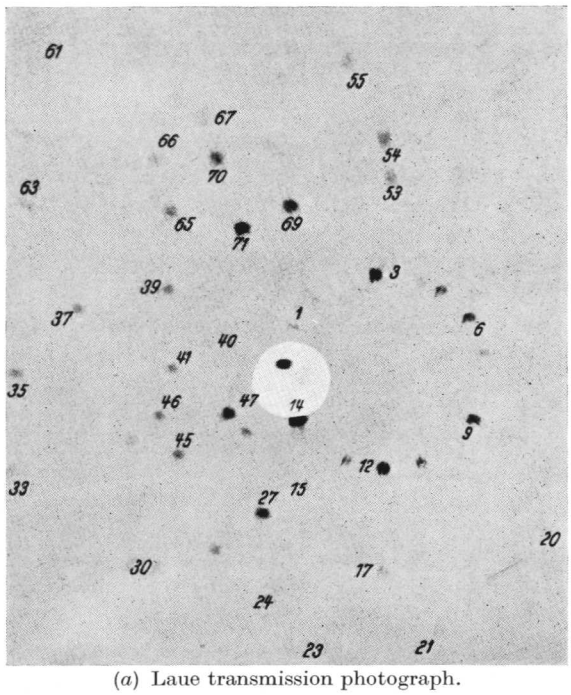

(*a*) Laue transmission photograph.

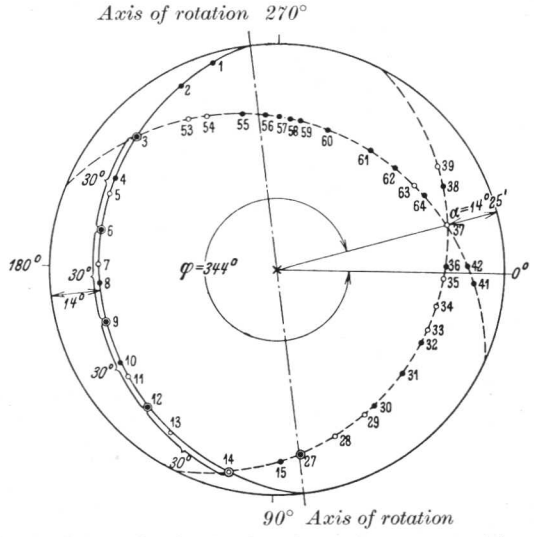

(*b*) Pole figure of the reflecting lattice planes (in stereographic projection).

FIG. 28 (*a*) and (*b*).—Determination of the Orientation of a Magnesium Crystal.

crystal to plates (Fig. 30). The normal N_1 or N_2 to the reflecting lattice planes lies in each case in the plane defined by the incident

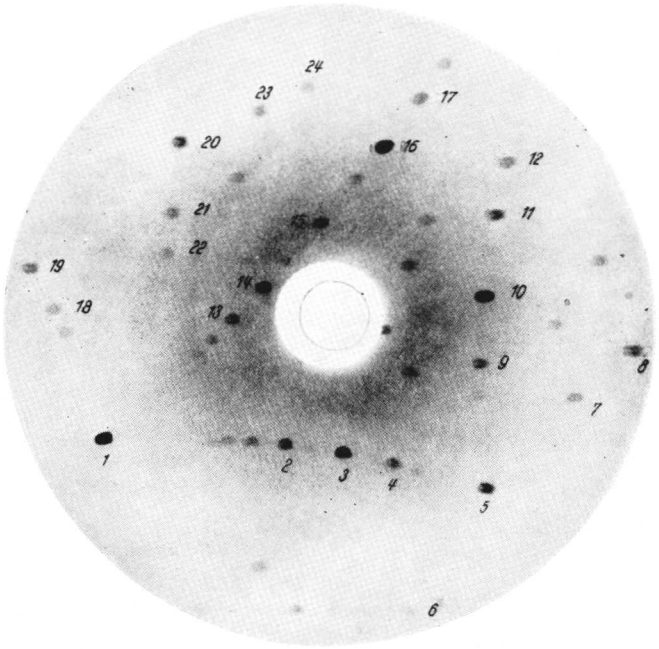

(*a*) Laue back-reflexion photograph.

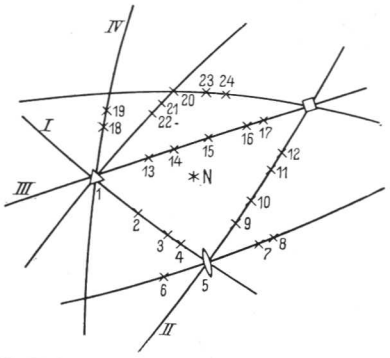

(*b*) Pole figure of the reflecting lattice planes (in stereographic projection).

FIG. 29 (*a*) and (*b*).—Determination of the Orientation of an Aluminium Crystal.

and diffracted beams and makes with the direct beam the angle $(90° - \theta_1/2)$ or $(90° - \theta_2/2)$. If now the position of the plane of

the two beams is defined by the angle, ϕ_1 or ϕ_2, which it makes with an arbitrarily selected plane of reference, then the pole of the

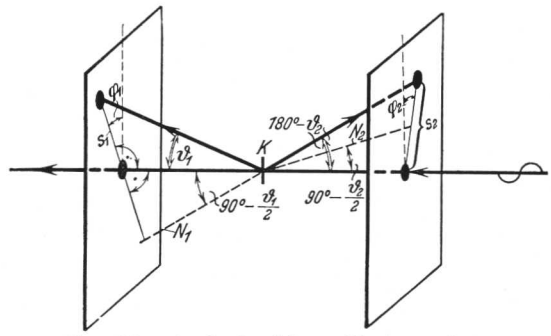

FIG. 30.—Analysis of Laue Photographs.

reflecting plane can be shown on a stereographic projection whose equatorial plane is the plane of the crystal plate.

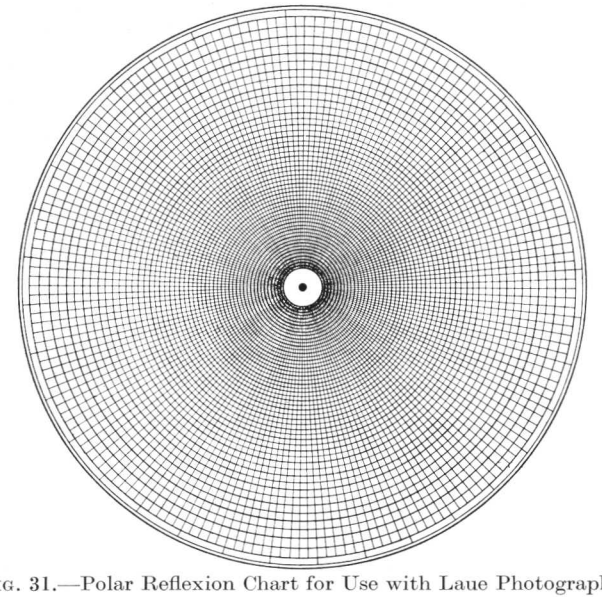

FIG. 31.—Polar Reflexion Chart for Use with Laue Photographs.

In order to simplify the determination of the θ-angles for the various reflexions it is convenient to employ a polar reflexion chart (Fig. 31) which indicates the θ-angles corresponding to the various S-values for a given plate distance (91). By superimposing Laue

photograph and chart, the θ and ϕ angles for all reflexions can be read off directly. If these are plotted in the stereographic projection, then the pole figure for all reflecting-lattice planes is obtained (Figs. 28*b* and 29*b*). As will be seen from Fig. 30 the angle $(90° - \theta/2)$ from the centre must be plotted in the direction of the corresponding reflexion for back-reflexion photographs, and in the *opposite* direction for transmission photographs.

The orientation can now be determined from these pole figures in two ways. By the first method the pole figure, in which the zones

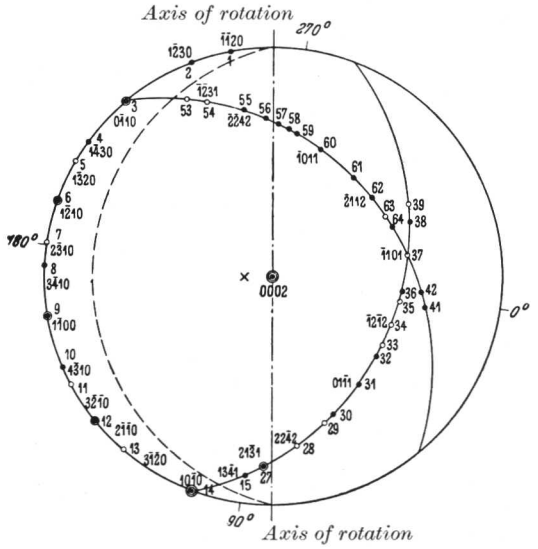

FIG. 32.—Determination of the Orientation of a Magnesium Crystal. Pole Figure of Fig. 28*b*, Rotated through 14°.

appear clearly as great circles passing through the reflexions, can be transformed into a pole figure corresponding to a simple setting of the crystal by rotation about an axis lying in the equatorial plane (the rotation method). By the second method the crystallographic description of the zones and plane normals can be derived directly from the relationship between the angles which appear on the stereographic pole figure.

For the first method we employ the pole figure of the transmission photograph (Fig. 28*b*) in which the intensity of the reflexions is also indicated. By rotating in such a way that the zone 1, 2 . . . 14 comes into coincidence with the basic circle, a pole figure (Fig. 32)

is obtained which coincides with the pole figure of the magnesium crystal about the hexagonal axis (Fig. 33).[1] As a consequence of this rotation the plate normal moves to X; its orientation, *i.e.*, the angles which it makes with the hexagonal and digonal axes, can be

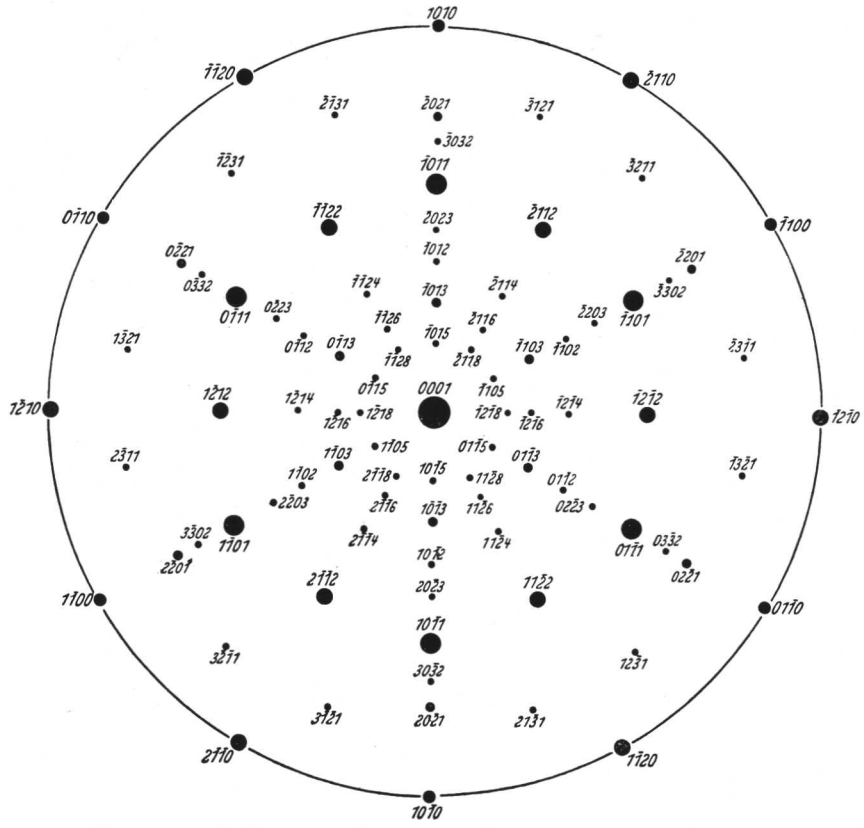

FIG. 33.—Pole Figure of Magnesium about the Hexagonal Axis (90).

seen from Fig. 32; they are $\rho = 14°$ with the hexagonal axis, and 77° and 76° with the nearest digonal axes of types I or II. If the longitudinal and transverse directions were also entered on the pole figure, the crystallographic orientations of these two directions would be immediately apparent.

[1] In this case the zone 1, 2 . . . 14 is seen to be a zone of the hexagonal axis from the fact that it exhibits reflexion angles of 30°.

Applying the second method to the stereographic figure in Fig. 29*b* we obtain the following angles between the important zones :

$$(\text{I–II}) = 90°; \quad (\text{I–III}) = 60°; \quad (\text{I–IV}) = 60°$$
$$(\text{II–III}) = 45°; \quad (\text{II–IV}) = 45°; \quad (\text{III–IV}) = 60°.$$

From this it follows that I, III, IV are zones of cube-face diagonals, while II is a cubic-axis zone. Zone intersections are represented by a cube edge (II–III), a face diagonal (I–II) and a body diagonal (I–III–IV). In this way the orientation of the normal (N) of the specimen which emerges from the centre of the net is fixed. It makes the angles 34°, 61° and 74° with the three cubic axes.

If the direction of incidence of the X-ray beam coincides with a symmetry axis of the crystal, the Laue photograph will exhibit a correspondingly symmetrical pattern. As a rule the nature of the symmetry of the Laue photograph suffices in this case to determine the crystallographic direction of the incident beam. Photographs obtained by the back-reflexion method are specially suitable for this purpose, besides having the additional advantage of being practicable with thick specimens [cf., *e.g.*, (92)].

Finally, it should be mentioned that atlases of the Laue photographs, obtained with face-centred cubic and body-centred cubic crystals by systematically varying the orientation, have been prepared (93).

CHAPTER V

GEOMETRY OF THE MECHANISMS OF CRYSTAL DEFORMATION

Before discussing in the second part of this book the results of investigations into crystal plasticity, we propose in the present chapter to examine the geometry of the various mechanisms of deformation in so far as it serves to explain the processes to be described.

It has long been known that crystals can be plastically deformed. The mechanisms which accompany plastic flow are based on the phenomena of glide (translation) and mechanical twinning (simple shear), which were discovered by Reusch on rock salt and calcite (1867). In both cases the deformation is plane and homogeneous, straight lines and planes remaining straight and plane; a sphere is transformed into an ellipsoid. The crystalline structure is also retained in the deformed part, the lattice being transformed into itself by the deformation.

A. GLIDE [1]

25. *Model of Gliding*

Glide consists in the slipping of portions of the crystal along crystallographic planes of low indices in the direction of densely packed atomic rows. Consequently neither the plane nor the direction of slip is determined by the loading (for instance, by a maximum of the shear stress); both these lattice elements are fixed by the structure of the lattice.

Fig. 34 shows the model of a cylindrical crystal which has been extended by glide (94). The model represents the basal glide of a hexagonal crystal under uni-axial tension. The upper and lower boundaries of the cylindrical specimen are made up of basal planes. The direction of glide is chosen to be a digonal axis of type I, and the hexagon sketched on the basal plane indicates that in general this glide direction does not coincide with the large elliptical axis. Glide along the crystallographically preferred glide system [2] leads

[1] Throughout this book the word "glide" has been used in preference to "slip". The terms are, however, synonymous and in the literature either may be used.

[2] The glide system that is mechanically preferred by a maximum of the shear stress consists, for uni-axial tension, of the plane that makes 45° with the axis of tension, and the major axis of the ellipse as the glide direction [cf., *e.g.* (40/1)].

to the configuration shown in Fig. 34, *c* and *d*. It is obvious that the change in shape produced in this way is quite specific (band formation) : the originally cylindrical crystal contracts considerably in one direction, while it expands somewhat in the direction perpendicular to it, owing to the divergence of the glide direction from the major axis of the translation ellipses. A comparison between Fig. 34, *b* and *d*, shows also that the extension has been accompanied

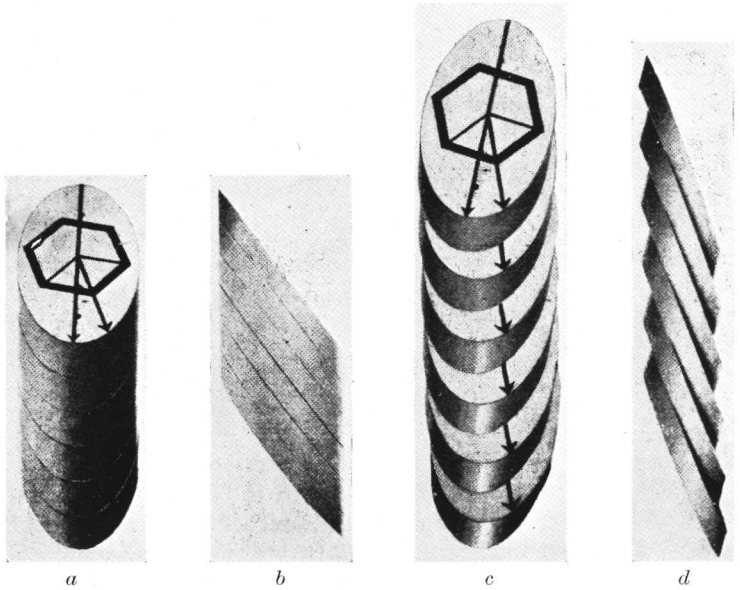

FIG. 34 (*a*)–(*d*).—Models of Gliding.
(*a*) and (*b*), initial state; (*c*) and (*d*), after extension.

by a very marked rotation of the lattice with respect to the longitudinal direction (direction of tension).

How closely this model corresponds to reality is shown by the photographs of elongated metal crystals reproduced in Fig. 35.[1] The traces of the glide planes appear as sharply defined elliptical bands on the surface of the strip. The position of the apex of the ellipses outside the central plane of the crystal band reveals clearly the divergence between glide direction and the major axis of the ellipses.

[1] For very early observations of glide bands and band formation resulting from the elongation of metal crystals see (95) and (96).

26. *Geometrical Treatment of Simple Glide*

The formulæ expressing the relationship between deformation and lattice rotation when a single-glide system is operative will be examined in the first place for *extension* with the aid of Fig. 36. The initially cylindrical crystal will be extended between the two glide planes that go through the points A and B respectively. Glide

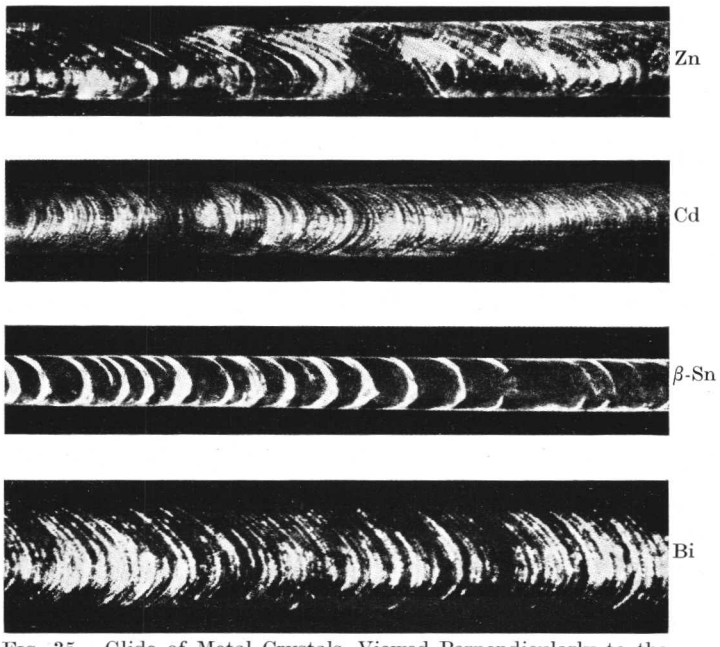

FIG. 35.—Glide of Metal Crystals, Viewed Perpendicularly to the Plane of the Band.

takes place parallel to the glide plane T in the glide direction t. The resultant configuration is drawn with thick lines; it has a double kink. It will again be seen from the diagram that the glide has been accompanied by lattice rotation relative to the longitudinal axis, although in this case it is the lattice position (position of the glide elements) and not, as in Fig. 34, the longitudinal axis which has been kept fixed. The angle between longitudinal axis and glide direction diminishes with increasing extension. It will now be seen from Fig. 36 that the lattice rotation consists in a movement of the longitudinal axis towards the glide direction, during which the longitudinal axis always remains in the plane

determined by its original position and the direction of glide. The relationship between the amount of extension: $\left(\delta = \frac{l_1 - l_0}{l_0}\right.$; l_0 and l_1 representing the length before and after extension) and the rotation of the lattice is obtained directly from the triangles ABB', ABN and $AB'N$ (94). The triangle ABB' gives

$$\frac{l_1}{l_0} = 1 + \delta = \frac{\sin \lambda_0}{\sin \lambda_1} \quad (26/1)$$

where λ_0 and λ_1 represent the angles between the direction of tension and the glide *directions* before and after extension.

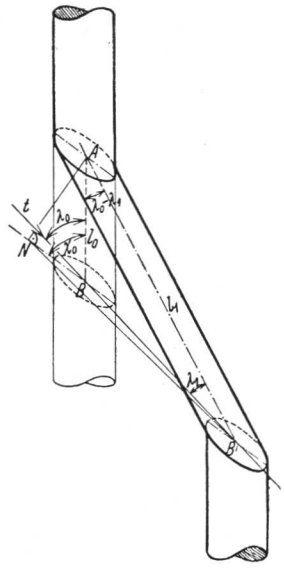

Fig. 36.—Diagram Illustrating the Formula for Extension by Gliding.

From the two right-angled triangles ABN and $AB'N$ (AN is the normal on the glide plane) we obtain for the small side AN common to both triangles the expressions

$$AN = l_0 \sin \chi_0 = l_1 \sin \chi_1$$

and further

$$\frac{l_1}{l_0} = 1 + \delta = \frac{\sin \chi_0}{\sin \chi_1} \quad (26/2)$$

in which χ_0 and χ_1 are the angles between glide *plane* and directions of tension before and after extension. It is seen from these formulæ that the amount of extension by glide can be very considerable; as a rule it will increase with the original obliquity of the glide elements to the direction of deformation.

The introduction of the *plastic shear strain* instead of the tensile strain has proved very convenient in the crystallographic analysis of stress–strain curves of crystals. This quantity, also known as the crystallographic glide strain (a), is the relative displacement of two glide planes of unit distance from each other [(97), (98)]. It is therefore given by the quotient $\frac{BB'}{AN}$; in which the numerator represents the total amount of slip and the denominator the thickness of the deformed glide packet. The connection between glide strain and extension can be easily derived from Fig. 36. For BB' we obtain from the triangle ABB'

$$BB' = \frac{l_1 \sin (\lambda_0 - \lambda_1)}{\sin \lambda_0}.$$